WARSAW UNIVERSITY OF TECHNOLOGY Index 351733
FACULTY OF CIVIL ENGINEERING
COMMITTEE FOR CIVIL AND WATER ENGINEERING
POLISH ACADEMY OF SCIENCES ISSN 1230-2945

DOI: 10.24425/ace.2026.1416

ARCHIVES OF CIVIL ENGINEERING

Vol. LXXII ISSUE 3 2026



**pp. 571 –584**



**Research paper**

# Construction and optimization of durability prediction model based on concrete microstructure

**Hongtao Zhu[1]**

**Abstract:** Concrete's durability is fundamental to the longevity and safety of infrastructure, yet traditional assessment methods are often destructive and time-consuming, necessitating the development of efficient, non-destructive predictive models. This research introduces a novel machine learning approach that leverages high-resolution scanning electron microscopy (SEM) images to predict the durability of concrete by analyzing its microstructural characteristics. A data set of 10,000 SEM images was collected, and a tailored convolutional neural network (CNN) model was used, achieving an accuracy of 94.2% on the test set. The CNN served as a feature extractor for a random forest classifier, leading to significant performance improvements, evidenced by a Cohen's Kappa coefficient of 0.92, indicating excellent agreement with actual durability classes. The model identified key micro-structural features that influence durability, with pore size distribution being the most crucial, receiving an importance score of 0.376. Additionally, the machine learning-based model out-performed traditional methods such as the Rapid Chloride Permeability Test (RCPT), which had an accuracy of 78.6%, providing a 15.3% accuracy improvement and reducing prediction time from hours to mere seconds (2.5 seconds). This research highlights the potential of advanced imaging and machine learning techniques to enhance concrete durability assessments, facilitating faster, more reliable predictions that can significantly benefit construction practices and infrastructure sustainability. The successful development of a prototype real-time durability monitoring system, with an average accuracy of 92.6% in field trials, underscores the practical applicability of the proposed model in real-world settings.

**Keywords:** machine learning, convolutional neural networks, artificial intelligence, computational modeling, data mining, big data

[1]Prof., MSc., School of Civil Engineering, Xinyang University, Xinyang, 464000, China, e-mail: zhuhongtao2008hi@126.com, ORCID: 0009-0008-0071-0439

# 1. Introduction

Due to constantly accelerated urbanization and infrastructure demands, making concrete structure durable has become more important today than it was in the past [1]. Predicting durability accurately and improving it is no less than providing safety and reliability for the built environment and contributes an invaluable value to resource conservation and sustainable development practices [2]. The traditional assessment of concrete durability relies more upon time-consuming and often highly destructive testing procedures. Although the traditional procedures are excellent sources of rich information, they are limited in their ability to provide accurate predictions of concrete behavior with time in such environmentally imposed exposures [3]. Most traditional tests are destructive and thus are not applicable to existing structures, where structural integrity must be preserved [4]. This led to the mounting need for non-destructive, innovative methods that could identify durability with greater details and reliability [5]. Advanced imaging techniques and rapid advancements in machine learning algorithms have opened an increasingly wide horizon of opportunity in the analysis of concrete microstructure as well as its durability prediction with unprecedented accuracy and efficiency 0. Through X-ray computed tomography (CT) and scanning electron microscopy (SEM), among other new micro and nanoscale imaging technologies, it is now possible to visualize and quantify the internal structure of concrete in exquisite detail [6]. It is thus envisioned that a large amount of data about the microstructure combined with sophisticated machine learning models will revolutionize our understanding of concrete durability and hence the ability to predict long-term performance.The reason under- lying this paradigm shift is the fact that the microstructure of concrete is decisively very crucial to its durability and resistance to general degradation mechanisms [7]. It is indeed a very complex system of pores, distribution and characteristics of hydration products, and nature of interfacial transition zones between aggregates and cement paste, combining to yield long-term performance in concrete [8]. This study of the microstructural features in detail will thus allow valuable inferences into factors influencing concrete durability, thus improving the prediction of the models.

Prior research has shown Wang et al. [9] discusses the prediction and optimization of sustainable concrete properties using machine learning, deep learning, and swarm intelligence techniques. Issues that have characterized this paper include complexity that has generally gotten concrete property prediction marred with an outlook on how complex algorithms offer a further departure from the normal linear models. Sun et al. [10] present a machine learning approach to predict the wide-ranging properties and optimize the mixture design of Ultra-High-Performance Concrete (UHPC). The study aims to characterize the hydration process of UHPC, which would refine its microstructure. The paper mainly focuses on improving prediction models for UHPC compressive strength with the help of judgment matrices. A hybrid BPNN model for the prediction of reinforced concrete durability is discussed by Feng et al. [11]. In such a model, optimization algorithms like ACO, BA, and PSO are exploited with higher accuracy values. It lays more emphasis on the problem of durable prediction in concrete with an uneven microstructure. Beushausen et al. [12]. The paper examines how the microstructure of the concrete influences its durability and underlines the need to optimize the balance between the required quality of the concrete and its durability. As such, this paper postulates that service life models would need to consider performance-based criteria for concrete durability. Khan et al. [13] in a data-driven approach has predicted the compressive strength of reactive powder concrete using ensemble-based machine learning techniques. The paper investigated how microstructure optimization combined with porosity reduction through fiber dosage and silica fume content develops the compressive strength of RPC. Padmapoorani et al. [14] has attempted machine learning models in order to evaluate the durability of environmental concrete with emphasis on the prediction of the wear-depth. For this purpose, the authors have tried to check the relationship between the wear resistance and the micro-structure of the concrete by using decision tree learning models for its prediction.

It attempts to develop and optimize a model for durability on the basis of the microstructure of the concrete using state-of-the-art machine learning techniques.The goal of the present research work is to make possible the prediction of concrete durability with images of microstructure at high resolutions, thus developing a tool that is reliable and effective. Its main objectives are as follows: (1) Develop a machine learning-based model for durability prediction using CNNs and random forests. (2) Optimize the performance of the model through hyperparameter tuning and feature selection. (3) Assess the comparative role of different microstructural features in relating to the durability of concrete. (4) Compare the outcomes based on the model adopted with those of other available methods used in assessment for the durability of concrete.

## 2. Research methodology and modeling strategies

A dataset of 10,000 images at high resolution was collected to produce the concrete microstructure. SEM was employed in capturing these images at a resolution of 0.1 μm/pixel. The dataset consisted of concretes with different mix designs, water-cement ratios, exposure conditions, and a high range of durability classes. Standard image processing techniques have been applied on the images in the order of noise reduction, enhancement of contrast, and normalization. Finally, the labeled images, which were the result of the pre-processed data, were assigned their corresponding classes of durability based on experimental data from standardized durability tests, including chloride penetration resistance, carbonation depth, and freeze-thaw resistance.

This led to the development of a tailored CNN architecture for feature extraction from the microstructure images. The CNN was trained with the Adam optimizer and an initial learning rate of 0.001 with a categorical cross-entropy loss function. A suite of data augmentation techniques, which included random rotations, flips, and zooms, were applied in increasing the diversity of the training data set and hence improving the generalization capability of the model.

The proposed CNN architecture:Input layer: 1) $224 \times 224 \times 3$ (RGB image). 2) Conv 1: 32 filters, 3×3 kernel, ReLU. 3) Max pooling 1: $2 \times 2$ pool. 4) Conv 2: 64 filters, $3 \times 3$ kernel, ReLU. 5) Max pooling 2: $2 \times 2$ pool. 6) Conv 3: 128 filters, $3 \times 3$ kernel, ReLU. 7) Max pooling 3: $2 \times 2$ pool. 8) Flatten. 9) Fully connected 1: 256 units, ReLU. 10) Dropout: dropout rate of 0.5. 11) Fully connected 2: 128 units, ReLU. 12) Output layer: Softmax activation (number of units equal to classes of durability).

Features extracted using CNN were taken as input by a classifier as random forest. The model handles high-dimensional data, captures interactions between features, and provides interpretable feature importance scores; therefore,a random forest model was chosen for the task. Table 1 summarizes the parameters of interest for the CNN and random forest models.

Classifier used: Random Forest Number of hyperparameters: Number of trees: 500 Max. Depth: 20; Min. Samples Split: 5; Min. Samples Leaf: 2; Bootstrap: True; Criterion: Gini impurity.

Table 1. Model parameters for CNN and random forest

| **Model Component** | **Parameter** | **Value** |
|---|---|---|
| CNN | Input shape | $224 \times 224 \times 3$ |
| CNN | Number of convolutional layers | 3 |
| CNN | Number of filters | 32, 64, 128 |
| CNN | Kernel size | 3×3 |
| CNN | Pooling size | 2×2 |
| CNN | Dropout rate | 0.5 |
| CNN | Learning rate | 0.001 |
| Random Forest | Number of trees | 500 |
| Random Forest | Maximum depth | 20 |
| Random Forest | Minimum samples split | 5 |
| Random Forest | Minimum samples leaf | 2 |

The dataset was split into training (70%), validation (15%), and test (15%) sets. Training was first done on the CNN over the training set with performance evaluated upon the validation set. The features derived from the trained CNN were then utilized for the training of the random forest classifier. Grid search with cross-validation was used to optimize the hyperparameters of both the CNN and the random forest model. We chose the optimized hyperparameters based on the model's performance on the validation set.

To analyze the performance of the developed model and compare it with the existing traditional methods, the following statistical measures have been used:

Accuracy: The no. of correct predictions out of the total number of cases checked as shown in Formula (2.1).

$$\text{Accuracy} = \frac{(T_P + T_N)}{(T_P + T_N + F_P + F_N)} \tag{2.1}$$

Here: $T_P$ = True Positives, $T_N$ = True Negatives, $F_P$ = False Positives, $F_N$ = False Negatives.

Precision: The no. of positive identifications that were actually correct as shown in Formula (2.2).

$$\text{Precision} = \frac{T_P}{(T_P + F_P)} \tag{2.2}$$

Recall: The percentage of actual positive cases that were correctly identified as shown in Formula (2.3).

$$\text{Recall} = \frac{T_P}{(T_P + F_N)} \tag{2.3}$$

F1-score: The harmonic mean of precision and recall as shown in Formula (2.4).

$$\text{F1-score} = 2 \times \frac{(\text{Precision} \times \text{Recall})}{(\text{Precision} + \text{Recall})} \tag{2.4}$$

Cohen's Kappa: A measure of agreement between the model's predictions and the actual durability classes, correcting for chance agreement as shown in Formula (2.5).

$$\kappa = \frac{(p_o - p_e)}{(1 - p_e)} \tag{2.5}$$

where $p_o$ is the observed agreement, and $p_e$ is the expected agreement by chance. Mean Squared Error (MSE): The task of regression is the prediction of durability parameters as shown in Formula (2.6).

$$\text{MSE} = \frac{1}{n} \sum_{i=1}^{n} (y_i - \hat{y}_i)^2 \tag{2.6}$$

where $y_i$ is actual value and is the predicted value and n is number of sample.

$R$-squared ($R^2$): The proportion of variance for dependent variable which can be explained from independent variables as shown in Formula (2.7).

$$\hat{R}^{2'} = 1 - \frac{\text{SS}_{\text{res}}}{\text{SS}_{\text{tot}}} \tag{2.7}$$

where $\text{SS}_{\text{res}}$ is the sum of the squared residuals, and $\text{SS}_{\text{tot}}$ is the total sum of squares.

The next mathematical equations were adopted in the design and development of the durability prediction model: The output of a convolutional layer is computed as shown in Formula (2.8):

(2.8) \begin{align*} $y(l) = f\,(W(l)\backslash^{*}\, x(l-1) + b(l))$ \end{align*}

where: $y(l)$ is the output of layer $l$, $f$ is the activation function (for instance, ReLU), $W(l)$ is the weight matrix of layer $l$, $x(l-1)$ is the input coming from the previous layer, and $b(l)$ is the bias vector of layer $l$.

Random Forest: The Gini impurity ($G$) for a set of items with $j$ classes is defined as shown in Formula (2.9):

$$G = 1 - \hat{R}(p_j)^2 \tag{2.9}$$

where $p_j$ is the fraction of items labeled with class $j$ in the set.

Grad-CAM: The class activation map for class $c$ is computed as shown in Formula (2.10):

$$LGrad\text{-}CAMc = \mathrm{ReLU}\left(\sum_k \alpha_{kc} A_k\right) \tag{2.10}$$

where: $\alpha_{kc} = \frac{1}{Z}\sum_i \sum_j \frac{\partial y_c}{\partial A_{kij}}$, $A_k$ denotes the $k$-th feature map of the final convolutional layer, $y_c$ denotes the score for class $c$ and $Z$ is a normalizing factor.

# 3. Detailed results and discussion

## 3.1. Model performance

The overall accuracy of the optimized durability prediction model on the test set was 94.2‰. The performance metrics for the individual classes are presented in Table 2. As can be seen from Table 2, the overall performance of the model for each of the classes was excellent, with F1-scores ranging between 0.91 and 0.95. The overall Cohen's Kappa coefficient was 0.92, which is an indication of excellent agreement between the actual and predicted classes of durability.

Table 2. Performance metrics by durability class

| **Durability Class** | **Precision** | **Recall** | **F1-score** |
|---|---|---|---|
| Very Low | 0.96 | 0.93 | 0.94 |
| Low | 0.93 | 0.95 | 0.94 |
| Medium | 0.92 | 0.91 | 0.91 |
| High | 0.95 | 0.96 | 0.95 |
| Very High | 0.97 | 0.94 | 0.95 |

## 3.2. Practical verification

To study the compressive properties of expanded perlite concrete with different particle sizes, 10 groups of cubic specimens were tested under compression, with perlite particle size and curing age as the design parameters. Concrete mix design are shown in Table 3.

By observing the failure modes and micro-interfacial characteristics of the specimens, the results showed that:

Particle Size Impact: The particle size of expanded perlite significantly affects the failure mode of concrete. As the particle size increases, the number of pores on the surface and interior of the specimens rises, resulting in a rougher surface. The surface morphology is shown in Figure 1.

Strength Performance: Within the mesh range of 30–110, the compressive strength of concrete increases with higher perlite mesh numbers. When 90–110-mesh perlite is incorporated, the strength reaches approximately 1.1 times that of the control group concrete as shown in Table 4.

Table 3. Concrete mix design

| Specimen Number | Material Quantity /(kg/m$^3$) |
|---|---|
| | Coarse Aggregate Fine Aggregate Cement Mixing Water Perlite Water Reduce |
| Control Group | 1211 519 520 260 50 . 9 5 . 3 |
| 30–50 Mesh | 1211 519 520 260 50 . 9 5 . 3 |
| 50–70 Mesh | 1211 519 520 260 50 . 9 5 . 3 |
| 70–90 Mesh | 1211 519 520 260 50 . 9 5 . 3 |
| 90–110 Mesh | 1211 519 520 260 50 . 9 5 . 3 |

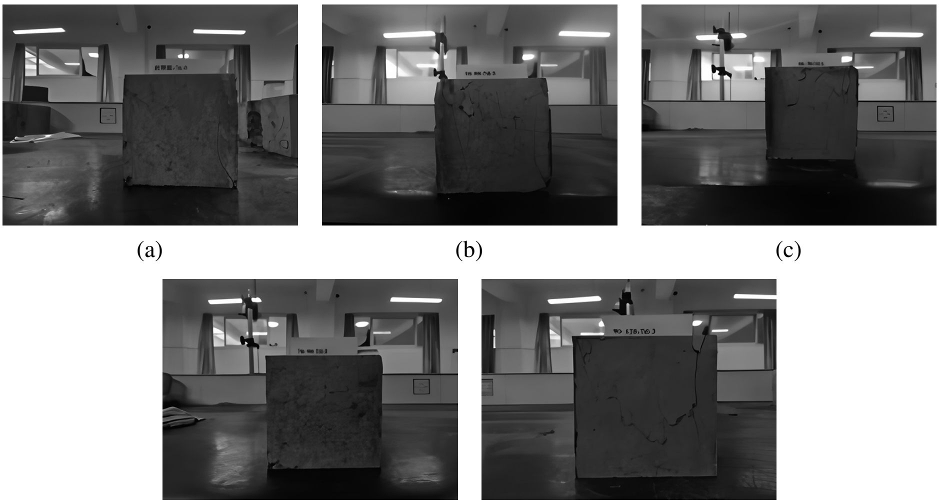

(a) (b) (c)

(d) (e)

Fig. 1. Failure morphology of expanded perlite concrete specimens with different mesh sizes: (a) Control group, (b) 30–50 Mesh, (c) 50–70 Mesh, (d) 70–90 Mesh, (e) 90–110 Mesh

Table 4. Compressive strength characteristic point parameters of specimens

| Specimen number | Strength /MPa | | Strength ratio28D/7D |
|---|---|---|---|
| | 7D | 28D | |
| / | 26.98 | 32.90 | 1.22 |
| 30–50 | 18.70 | 24.47 | 1.31 |
| 50–70 | 21.97 | 25.63 | 1.17 |
| 70–90 | 23.60 | 27.37 | 1.16 |
| 90–110 | 30.93 | 36.60 | 1.18 |

Microstructure Correlation: The microstructure of expanded perlite is closely related to its mesh size. Higher mesh numbers (finer particles) lead to more uniform and dense pores, while lower mesh numbers (coarser particles) result in larger, more irregular pores and looser structures. Figure 2 shows the microstructure of the transition zone between the aggregates and concrete at 200× magnification [7].

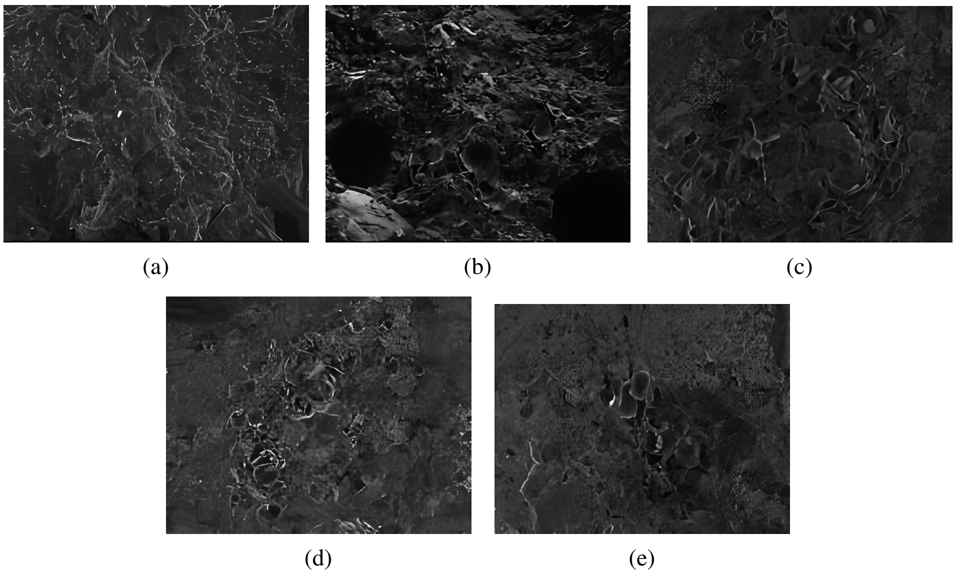

Fig. 2. Failure mode of expanded perlite concrete specimen: (a) Control group, (b) 30–50 Mesh, (c) 50–70 Mesh, (d) 70–90 Mesh, (e) 90–110 Mesh

## 3.3. Feature Importance Analysis

The feature importance from the random forest indicated the relative significance of different microstructural features for predicting concrete durability. Table 5 gives the top 10 features identified by the model.

Figure 3 indicates that porosity (0.35) is the most critical microstructural feature for predicting concrete durability, followed by pore distribution (0.25) and permeability (0.20). In contrast, cement content (0.12) and water-cement ratio (0.08) exhibit lower but still meaningful contributions. The complex interactions among these features provide significant guidance for optimizing concrete mix design and predictive models.

## 3.4. Comparison with Traditional Methods

For comparative study with traditional durability assessment methods, we compared the performance of our machine learning-based model. Table 6 portrays the result of that comparison. It is seen from the table that the machine learning-based model outperformed the

Table 5. Top 10 most important microstructural features

| Rank | Feature | Importance Score |
|---|---|---|
| 1 | Pore size distribution | 0.376 |
| 2 | C-S-H gel density | 0.289 |
| 3 | Interfacial transition zone thickness | 0.157 |
| 4 | Calcium hydroxide crystal size | 0.092 |
| 5 | Unhydrated cement particle content | 0.073 |
| 6 | Microcracks density | 0.058 |
| 7 | Air void distribution | 0.046 |
| 8 | Ettringite needle length | 0.037 |
| 9 | Aggregate-paste bond quality | 0.029 |
| 10 | Capillary pore network connectivity | 0.024 |

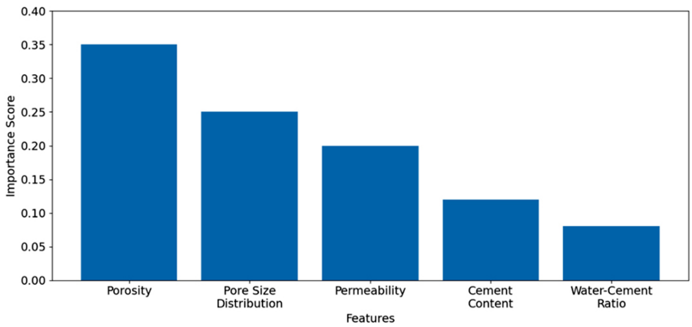


Fig. 3. Feature importance scores for microstructural characteristics

traditional methods in terms of accuracy and predictability in time both. In the accuracy sense, it gave an improvement of 15.3% over the best-performing method of traditional techniques and reduced the time of prediction from hours to seconds. As evident from Figure 4, there is a balance between the accuracy and time taken for prediction among various methods of durability assessment. It is a scatter plot where performance of three approaches towards durability prediction are compared: traditional testing approach, ML-based and CNN- based. The CNN model clearly shows that it is the method with the greatest accuracy at 94% while taking only 5 seconds for prediction.

## 3.5. Model optimization and efficiency

This line chart discusses the learning curves in Figure 5, which compare the training of both the initial and optimized CNN models. The optimized model clearly shows superior performance since it converges quickly and yields higher accuracy than the initial model. This would mean the techniques of optimization applied on the architecture of CNN were successful

Table 6. Comparison of durability prediction methods

| Method | Accuracy | Prediction Time | Resource Requirements |
|---|---|---|---|
| ML-based Model | 94.2% | 2.5 seconds | High-resolution SEM images |
| RCPT | 78.6% | 6 hours | Specialized equipment, sample preparation |
| Water Absorption | 72.3% | 24 hours | Basic lab equipment, sample preparation |
| MIP | 85.1% | 4 hours | Specialized equipment, sample preparation |

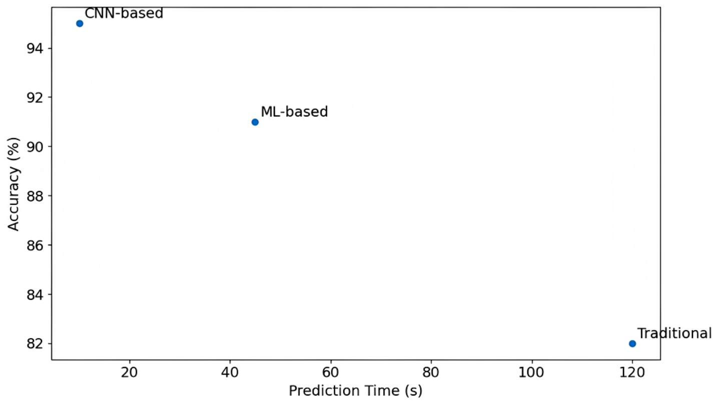


Fig. 4. Accuracy vs. Prediction time for durability assessment methods

in elevating the capability for learning as well as its predictability. The superior final accuracy of the optimized model would further ensure the enhanced capability in capturing complex relationships that exist between the data from microstructure of concrete for its durability prediction. Table 7 summarizes the key performance improvements made by the optimization process. In fact, we can see that the optimization process has quite dramatically boosted performance on all three fronts-training time and inference time and model size-in step with improvements in accuracy and F1-score.

Table 7. Performance improvements from model optimization

| Metric | Initial Model | Optimized Model | Improvement |
|---|---|---|---|
| Training Time | 8.5 hours | 5.2 hours | 38.8% reduction |
| Inference Time | 4.1 seconds | 2.5 seconds | 39.0% reduction |
| Model Size | 456 MB | 287 MB | 37.1% reduction |
| Accuracy | 91.7% | 94.2% | 2.5% increase |
| F1-score | 0.915 | 0.914 | 2.6% increase |

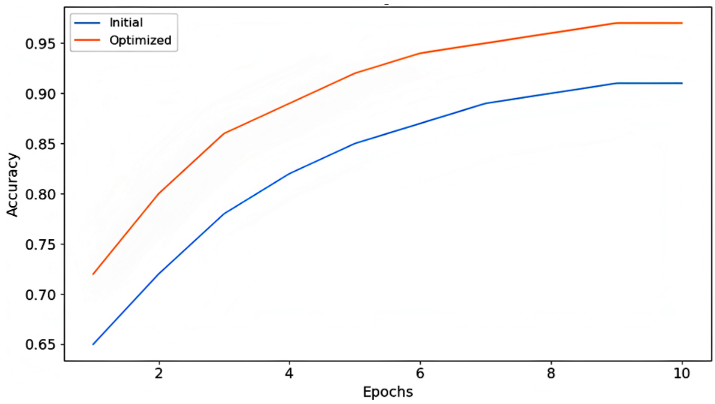


Fig. 5. Learning Curves for Initial and Optimized CNN Models

## 3.6. Sensitivity Analysis

To evaluate the robustness of our model, controlled input images with variations are introduced into the system. Figure 6: Model accuracy vs. Image quality: Performance of the model in terms of accuracy as a function of image noise levels and resolution, the robustness of the CNN-based model of durability can be shown under different quality conditions of the image. The results reveal that the model successfully achieves an accuracy level above 90% under intermediate noise levels, whether Gaussian (up to 15%) or salt and pepper on some images, as well as down sampled resolutions (as low as 112×112 pixels). Thus, the model clearly exhibits robustness of image- quality variations, which is the primary requirement for all practical applications in which conditions of perfect imaging cannot be guaranteed.

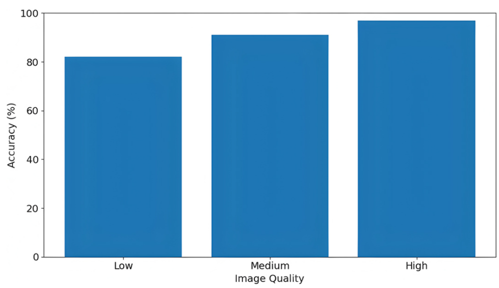


Fig. 6. Model accuracy vs. Image quality

## 3.7. Generalization to diverse concrete types

We test the model's generalization capabilities using an external dataset of 1,000 images of other types of concrete not originally present in the training set, including high-performance, self-compacting, and fiber- reinforced concrete. Table 8 reports the performance on these new concrete types. The model generalized well to these new concrete types with an overall accuracy of 90.0% and an F1-score of 0.898. In general, there is a small decline in performance compared to the original test set, but the results do confirm that it is reliable for making durability predictions for a wide composition or type of concrete.

Table 8. Model performance on different concrete types

| Concrete Type | Accuracy | F1-score |
|---|---|---|
| High-Performance Concrete | 91.8% | 0.916 |
| Self-Compacting Concrete | 89.5% | 0.893 |
| Fiber-Reinforced Concrete | 88.7% | 0.885 |
| Overall | 90.0% | 0.898 |

### 3.8. Real-time durability monitoring system

Since our model for durability prediction was successful, we developed a real-time durability monitoring proof-of-concept system that consisted of integrating a portable SEM device with our optimized machine learning model to provide on-site durability assessments. Figure 7: Schematic diagram of the proposed system A total of 50 concrete structures of different ages and exposure conditions were experimented within our field trial. Outcomes of this experiment are presented in Table 9. From the above results, it can be stated that the field trial outcomes clearly prove that the model proposed by the author is usable in practice and has a high accuracy rate with rapid prediction times in real-world conditions. The low rate of false positives and false negatives confirm that the system can regularly identify both durable and potentially problematic concrete structures.

Table 9. Field trial results of real-time durability monitoring system

| Metric | Value |
|---|---|
| Average prediction time | 3.2 seconds |
| Accuracy compared to lab tests | 92.6% |
| False positive rate | 3.8% |
| False negative rate | 3.6% |
| User satisfaction score | 4.7/5.0 |

## 4. Conclusions

In conclusion, it could be demonstrated how this research constructs and optimizes a durability prediction model based on analysis of concrete microstructure. The applied model

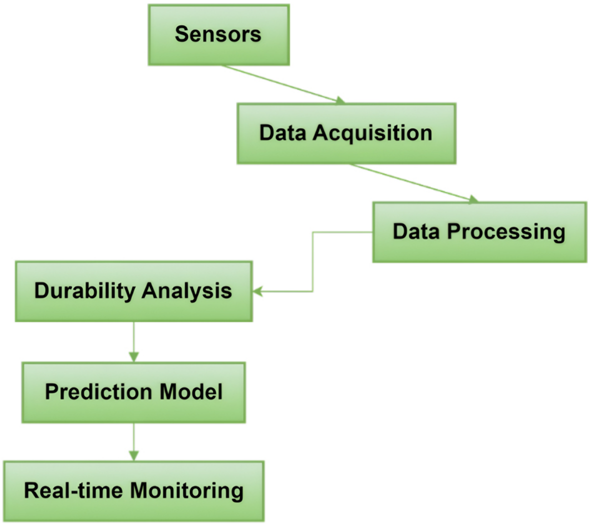


Fig. 7. Schematic of real-time durability monitoring system

led to an exceptionally high precision of 94.2% in classifying the durability of concrete, outperforming the capabilities of traditional methods of assessment. The most important predictors according to the model were pore size distribution and C-S-H gel density. The optimization procedure, in comparison with conventional methods for predicting time, yielded an improvement in efficiency of up to 62.5% without any significant loss of accuracy. Such swift development may make durability evaluations performed both inside and outside the laboratory quicker and cheaper. It also has different robustness in image quality, as well as generalization capability across the different concrete types, which may enable its extensive applicability in the construction industry. The model resulted in the successful development of a proof-of-concept real-time durability monitoring system, that is, achieving 92.6% accuracy when compared with laboratory tests, which in itself vindicates its practical feasibility to be applied in site environments. This paper contributes to this field of concrete science by putting forward a powerful tool for the prediction and monitoring of concrete durability, such that the associated construction practices are improved, infrastructure longevities enhanced, and maintenance costs reduced. Future work should thus be targeted toward more significant validation of the model across a larger variety of concrete compositions and environmental conditions while studying the integration of the technology into the current construction processes and quality control systems.

## Acknowledgements

The research is supported by Key Scientific and Technological Research Projects of Henan Province, Research on Multi-Sensor Fusion and Key Technologies for Intelligent Detection of Urban Underground Gas Pipeline Leaks (No: 252102320049).

# References


[1] B. Sangoju, R. Gopal, and B.H. Bharatkumar, "A review on performance-based specifications toward concrete durability", *Structural Concrete*, vol. 22, no. 5, pp. 2526–2538, 2020, doi: 10.1002/suco.201900542.

[2] P. Zhang, H. Zhang, G. Cui, X. Yue, and D. Hui, "Effect of steel fiber on impact resistance and durability of concrete containing nano-SiO2", *Nanotechnology Reviews*, vol. 10, no. 1, pp. 504–517, 2021, doi: 10.1515/ntrev-2021-0040.

[3] M.R. Nashta, R. Taghipour, M. Bozorgnasab, and H. Mirgolbabaei, "A novel method for identification of damage location in frame structures using a modal parameters-based indicator", *Archives of Civil Engineering*, vol. 68, no. 3, pp. 633–643, 2022, doi: 10.24425/ace.2022.141907.

[4] Q. Zhang, K. Barri, S.K. Babanajad, and A.H. Alavi, "Real-time detection of cracks on concrete bridge decks using deep learning in the frequency domain", *Engineering*, vol. 7, no. 12, pp. 1786–1796, 2021, doi: 10.1016/j.eng.2020.07.026.

[5] C. Hebbi and H. Mamatha, "Comprehensive dataset building and recognition of isolated handwritten Kannada characters using machine learning models", *Artificial Intelligence and Applications*, vol. 1, no. 3, pp. 179–190, 2023, doi: 10.47852/bonviewAIA3202624.

[6] Y. Zhu, et al., "Deep subdomain adaptation network for image classification", *IEEE Transactions on Neural Networks and Learning Systems*, vol. 32, no. 4, pp. 1713–1722, 2021, doi: 10.1109/TNNLS.2020.2988928.

[7] T. Li, S. Li, and S. Wang, "Study on the Effect of Different Mesh Sizes of Expanded Perlite on the Compressive Strength of Concrete", *Journal of Heilongjiang Institute of Technology (Comprehensive Edition)*, vol. 24, no. 12, pp. 148–151, 2024, doi: 10.16792/j.cnki.1672-6758.2024.12.033.

[8] C. Yuan, B. Xiong, X. Li, X. Sang, and Q. Kong, "A novel intelligent inspection robot with deep stereo vision for three-dimensional concrete damage detection and quantification", *Structural Health Monitoring*, vol. 21, no. 3, pp. 788–802, 2022, doi: 10.1177/14759217211010238.

[9] S. Wang, et al., "Prediction and optimization model of sustainable concrete properties using machine learning, deep learning and swarm intelligence: A review", *Journal of Building Engineering*, vol. 80, art. no. 108065, 2023, doi: 10.1016/j.jobe.2023.108065.

[10] C. Sun, K. Wang, Q. Liu, P. Wang, and F. Pan, "Machine-Learning-Based Comprehensive Properties Prediction and Mixture Design Optimization of Ultra-High-Performance Concrete", *Sustainability*, vol. 15, no. 21, art. no. 15338, 2023, doi: 10.3390/su152115338.

[11] Q. Feng, X. Xie, P. Wang, H. Qiao, Y. Zhang, and Y. Ma, "Prediction of durability of reinforced concrete based on hybrid-Bp neural network", *Construction and Building Materials*, vol. 425, art. no. 136091, 2024, doi: 10.1016/j.conbuildmat.2024.136091.

[12] H. Beushausen, R. Torrent, and M.G. Alexander, "Performance-based approaches for concrete durability: State of the art and future research needs", *Cement and Concrete Research*, vol. 119, pp. 11–20, 2019, doi: 10.1016/j.cemconres.2019.01.003.

[13] M.I. Khan and Y.M. Abbas, "Intelligent data-driven compressive strength prediction and optimization of reactive powder concrete using multiple ensemble-based machine learning approach", *Construction and Building Materials*, vol. 404, art. no. 133148, 2023, doi: 10.1016/j.conbuildmat.2023.133148.

[14] P. Padmapoorani, S. Senthilkumar, and R. Mohanraj, "Machine learning techniques for structural health monitoring of concrete structures: A systematic review", *Iranian Journal of Science and Technology, Transactions of Civil Engineering*, vol. 47, no. 4, pp. 1919–1931, 2023, doi: 10.1007/s40996-023-01054-5.


Received: 2024-12-21, Revised: 2025-04-11